Dalton 09-04—George Britovsek

VG0149 ([Fe(**1**)(OTf)$_2$]**), VG0150 (**[Fe(**1**)(OTf)(CH$_3$CN)](SbF$_6$)**), GB0301 (**[Fe(**2**)(CH$_3$CN)$_3$](SbF$_6$)$_2$**), GB0201 (**[Ru(**2**)(CH$_3$CN)$_3$](SbF$_6$)$_2$**), GB0205 (**[Mn(**2**)(OTf)$_2$(H$_2$O)]**)**

Supplementary Data — X-Ray Crystallography for B414813D

Manuscript:	Synthesis of iron(II), manganese(II), cobalt(II) and ruthenium(II) complexes containing tridentate nitrogen ligands and their application in the catalytic oxidation of alkanes
Authors:	George J.P. Britovsek, Jason England, Stefan K. Spitzmesser, Andrew J.P. White and David J. Williams

Fig. S1	The molecular structure of one (**B**) of the two independent molecules present in the crystals of [Ru(**2**)(CH$_3$CN)$_3$](SbF$_6$)$_2$.
Fig. S2	The molecular structure of [Fe(**1**)(OTf)$_2$] (30% probability ellipsoids).
Fig. S3	The molecular structure of [Fe(**1**)(OTf)(CH$_3$CN)](SbF$_6$) (30% probability ellipsoids).
Fig. S4	The molecular structure of [Fe(**2**)(CH$_3$CN)$_3$](SbF$_6$)$_2$ (50% probability ellipsoids).
Fig. S5	The molecular structure of one (**A**) of the two independent molecules present in the crystals of [Ru(**2**)(CH$_3$CN)$_3$](SbF$_6$)$_2$ (30% probability ellipsoids).
Fig. S6	The molecular structure of one (**B**) of the two independent molecules present in the crystals of [Ru(**2**)(CH$_3$CN)$_3$](SbF$_6$)$_2$ (30% probability ellipsoids).
Fig. S7	The molecular structure of [Mn(**2**)(OTf)$_2$(H$_2$O)] (50% probability ellipsoids).
Fig. S8	DQF-COSY ^{1}H-NMR spectrum of the paramagnetic complex [Fe(**1**)Cl$_2$] in CD$_2$Cl$_2$.

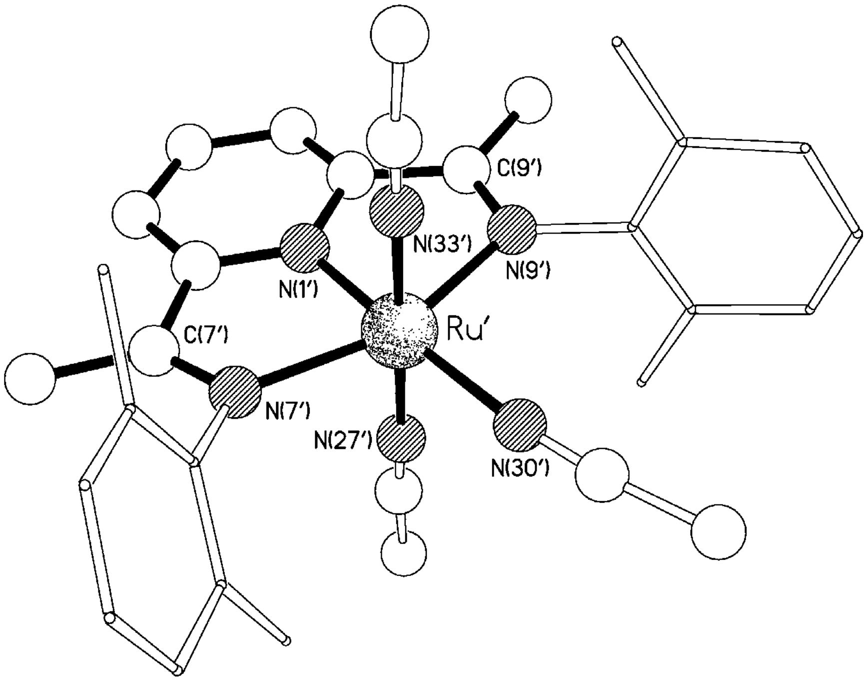
C(9′)
N(33′)
N(9′)
N(1′)
Ru′
C(7′)
N(7′)
N(27′)
N(30′)

Fig. S1

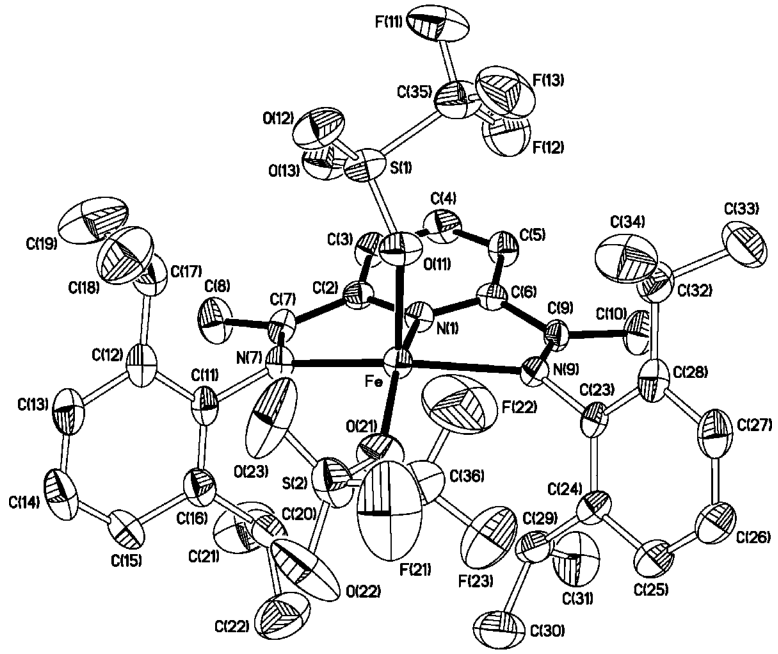
F(11)
F(13)
C(35)
O(12)
F(12)
O(13)
S(1)
C(4)
C(34)
C(33)
C(3)
C(5)
C(19)
O(11)
C(17)
C(18)
C(8)
C(7)
C(2)
C(6)
C(32)
C(9)
C(10)
N(1)
C(12)
N(7)
C(11)
Fe
N(9)
C(28)
C(13)
C(23)
F(22)
O(21)
C(27)
O(23)
S(2)
C(36)
C(14)
C(16)
C(20)
C(24)
C(29)
C(26)
C(21)
C(15)
F(21)
F(23)
C(31)
C(25)
O(22)
C(22)
C(30)

Fig. S2

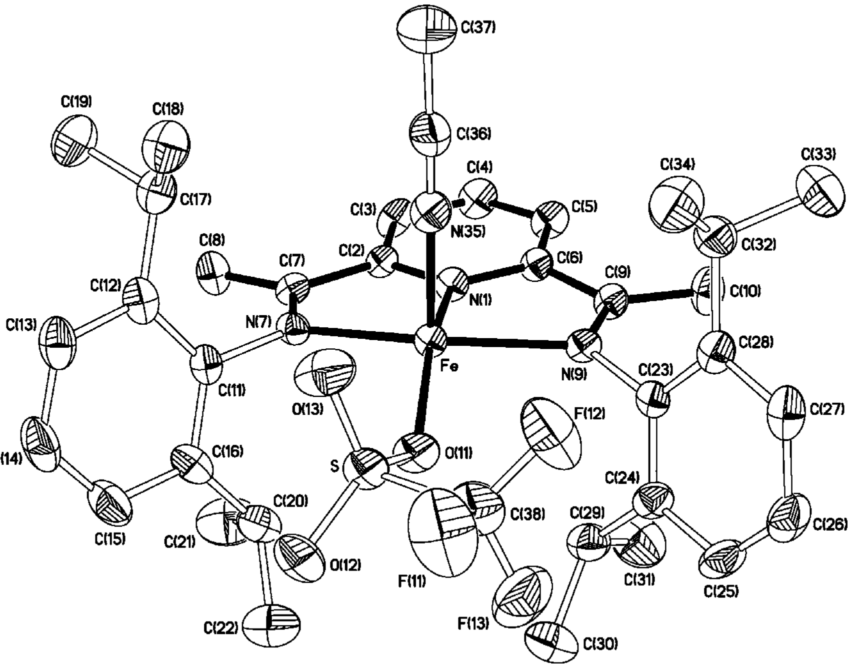
C(37)
C(19)
C(18)
C(36)
C(34)
C(33)
C(4)
C(17)
C(3)
C(5)
N(35)
C(32)
C(8)
C(2)
C(6)
C(7)
C(9)
N(1)
C(12)
C(10)
C(13)
N(7)
C(28)
Fe
N(9)
C(23)
C(11)
C(27)
O(13)
F(12)
C(14)
C(16)
O(11)
S
C(24)
C(20)
C(38)
C(29)
C(26)
C(15)
C(21)
O(12)
C(31)
F(11)
C(25)
F(13)
C(22)
C(30)

Fig. S3

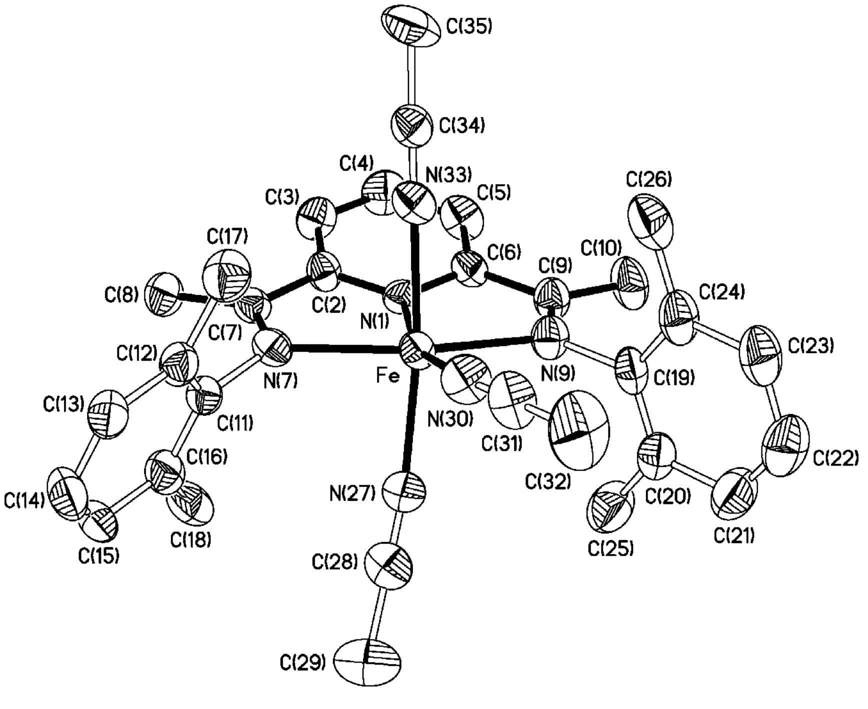
C(35)
C(34)
C(4)
N(33)
C(26)
C(3)
C(5)
C(6)
C(10)
C(17)
C(9)
C(24)
C(8)
C(2)
N(1)
C(7)
C(12)
N(7)
Fe
N(9)
C(19)
C(23)
C(13)
C(11)
N(30)
C(31)
C(16)
C(22)
C(14)
N(27)
C(32)
C(20)
C(15)
C(18)
C(25)
C(21)
C(28)
C(29)

Fig. S4

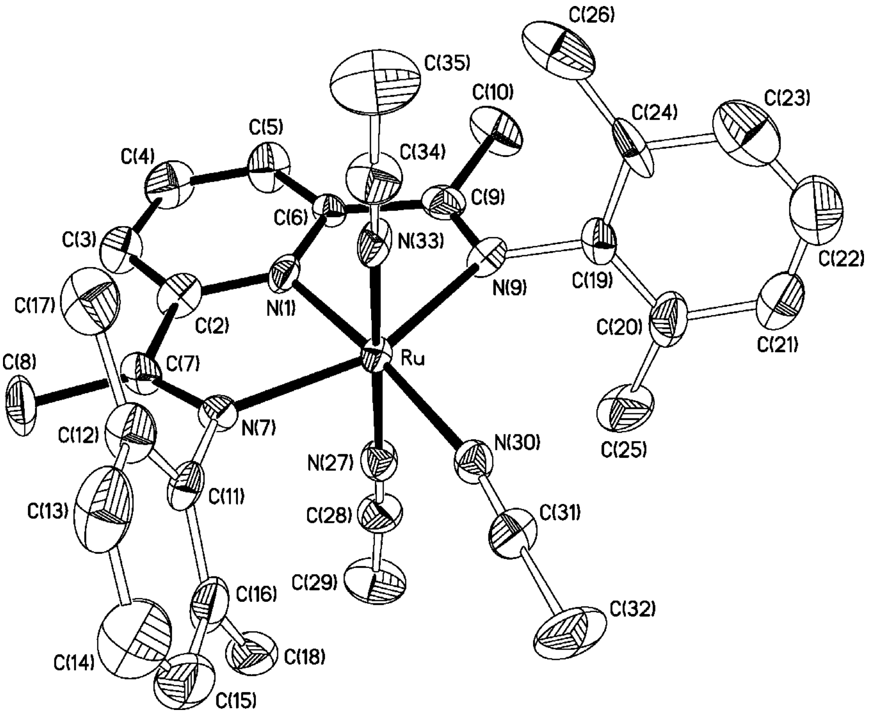
C(26)
C(35)
C(10)
C(24)
C(23)
C(5)
C(4)
C(34)
C(9)
C(6)
C(3)
N(33)
C(22)
N(9)
C(19)
C(17)
C(2)
N(1)
C(20)
C(21)
C(7)
Ru
C(8)
C(12)
N(7)
C(25)
N(27)
N(30)
C(11)
C(13)
C(28)
C(31)
C(29)
C(16)
C(32)
C(14)
C(18)
C(15)

Fig. S5

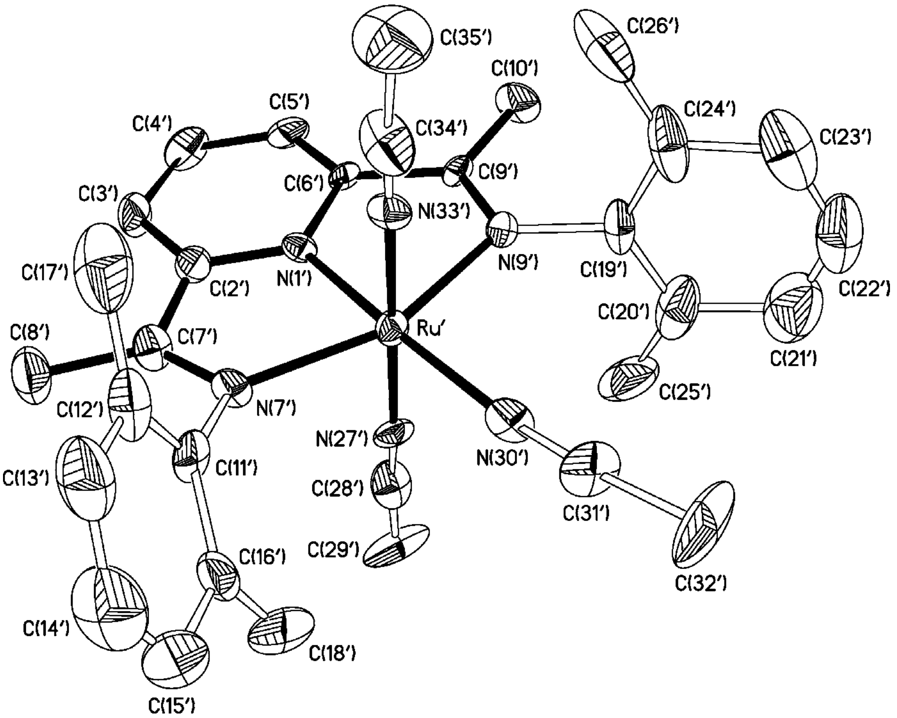
C(35')
C(26')
C(10')
C(5')
C(24')
C(4')
C(34')
C(23')
C(9')
C(6')
C(3')
N(33')
N(9')
C(19')
C(17')
C(2')
N(1')
C(22')
C(20')
C(8')
C(7')
Ru'
C(21')
C(25')
C(12')
N(7')
N(27')
N(30')
C(11')
C(13')
C(28')
C(31')
C(29')
C(16')
C(32')
C(14')
C(18')
C(15')

Fig. S6

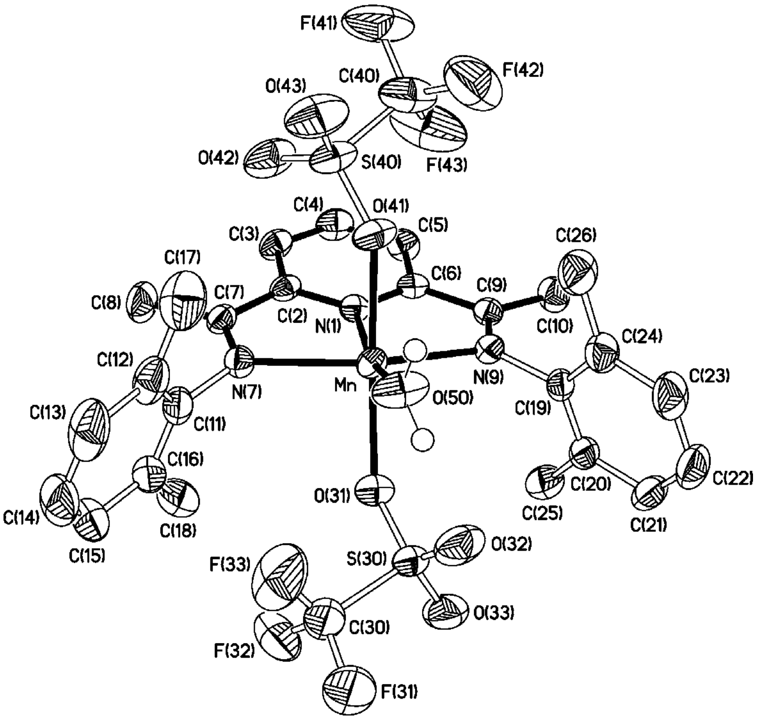
F(41)
C(40)
F(42)
O(43)
O(42)
S(40)
F(43)
C(4)
O(41)
C(5)
C(3)
C(26)
C(17)
C(6)
C(9)
C(8)
C(7)
C(2)
N(1)
C(10)
C(24)
C(12)
Mn
N(9)
C(23)
N(7)
O(50)
C(19)
C(13)
C(11)
C(16)
C(22)
O(31)
C(20)
C(14)
C(25)
C(21)
C(18)
O(32)
C(15)
S(30)
F(33)
O(33)
C(30)
F(32)
F(31)

Fig. S7

Figure S8 depicts the DQF-COSY paramagnetic ^{1}H-NMR spectrum of complex [Fe(**1**)Cl$_2$] in CD$_2$Cl$_2$. Although the one-dimensional ^{1}H NMR spectrum appears as singlets only, cross peaks are clearly visible in the DQF-COSY spectrum, revealing the coupling between the *meta* and *para* pyridyl protons A and B and the *meta* and *para* phenyl protons C and D, thus making these peak assignments unambiguous. No coupling between the isopropyl methyl protons at $\delta =$ –5.3 and –6.3 ppm and the methine protons at $\delta =$ –22.4 ppm, probably due to the severe broadening of the latter. These signals are therefore considered as singlets and disappear from the diagonal, as do the ligand backbone methyls at $\delta =$ –37.1 ppm. The signals in the diamagnetic region are due to solvent residues (thf and dcm).

Figure S8